Langmuir

Article

pubs.acs.org/Langmuir

# Molecular Packing of Amphipathic Peptides on the Surface of Lipid Membranes

Christopher Aisenbrey* and Burkhard Bechinger

Institut de Chimie, UMR7177, Université de Strasbourg/CNRS, 1, rue Blaise Pascal, 67000 Strasbourg, France

Supporting Information

**ABSTRACT:** When polypeptides bind to the membrane surface, they become confined to a restricted quasi-two-dimensional space where peptide−peptide interactions become highly relevant, and the concept of a crowded medium is appropriate. Within this crowded environment interesting effects like clustering, separation of phases, cooperative alignment, and common movements occur. Here we investigated such effects by measuring distances between fluorophore-labeled peptides in the range ≤1 nm by fluorescence self-quenching. For helical peptides with dimensions of approximately 1 × 3 nm such a small "ruler" is sensitive to the packing of the labeled peptides and thereby to their molecular arrangement. A novel approach to characterize peptide−peptide interactions within membranes is presented using the designer peptide LAH4. This sequence changes membrane topology in a controlled manner being transmembrane at neutral conditions but oriented parallel to the surface at low pH. Experimental measurements of the fluorescence self-quenching of close-by chromophores and the changes that occur upon dilution with unlabeled peptides are used to analyze the peptide distribution within the membrane surface. The data show a strong effect of electrostatic interactions and under some experimental conditions clustering of the peptides. Furthermore, the results suggest that at pH 4 the peptides arrange along the membrane surface in an ordered mesophase-like arrangement.

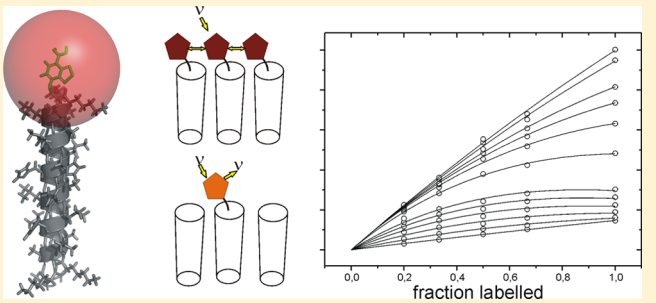


## INTRODUCTION

The fluid mosaic model by Singer and Nicolson[1] dominates our view of lipid membranes as two-dimensional liquids. However, at high concentrations the finite size of peptides and proteins incorporated into lipid membranes results in the crowding of these macromolecules and thereby a more ordered (mosaic) structure in the membrane.[2] Theoretical considerations suggest the existence of anisotropic (mesomorphic) phases of rod-shaped peptides at the membrane surface.[3] Such arrangements may be important for the function and regulation of membrane-based processes, and a better description of the packing of peptides and proteins within the membrane is essential for our understanding. In addition, peptides residing at the membrane surface represent a tractable model system to investigate the behavior of scaled particles of different shape in two dimensions, thereby introducing concepts from surface physics and chemistry to membrane biophysics.

Molecular crowding at the membrane occurs at high peptide concentrations, but its influence on the adsorption isotherms was investigated theoretically and experimentally in only a few publications.[3−7] The study presented here extends these previous experiments by developing a microscopic picture, where the focus is on the packing of peptides on the lipid bilayer surface. The LAH4 peptide (KKALL ALALH HLAHL ALHLA LALKK A) was investigated as, depending on the pH of the environment, it can adopt both in-planar and transmembrane configurations.[8] The pH-dependent topology is based on the protonation of its four histidines that exhibit p$K$ values in the range 5.4−6.[8] At low pH the protonated/cationic histidines ensure that the resulting highly amphipathic helical structure adopts an orientation with its long axis parallel to the membrane surface. In contrast, at neutral pH hydrophobic interactions dominate and the uncharged histidines insert into the membrane; thus a transmembrane alignment of the peptide is obtained. The LAH4 peptide thereby allows one to compare these very different situations without changes in its amino acid sequence. Notably, the LAH4 peptides are not only of interest in academic grounds but also because of their biological activities, which they share with other cationic amphipathic peptides. The LAH4 sequences exhibit potent antimicrobial activities[9] and have been developed for nonviral transfection of DNA,[10] RNA,[11] polypeptides,[12] and quantum dots[13] as well as for the enhancement of viral transduction.[14]

In order to monitor the distribution of the peptides within the membranes, the self-quenching of NBD-fluorophores was used to reveal the close proximity between membrane-associated peptides. Self-quenching of fluorescence molecules can be described by statistical traps of close chromophores,[15−17] where the fluorescence excitation relaxes quickly due to the dipole−dipole coupling between the chromophores.

Received: March 14, 2014
Revised: August 7, 2014

   dx.doi.org/10.1021/la500998g | Langmuir XXXX, XXX, XXX−XXX

In the two-dimensional case the problem can be reduced to a two-particle system up to very high concentrations.[18] The self-quenching of NBD is characterized by a critical radius of 10 Å,[19] i.e., in the order of the dimensions of the peptide. To characterize the self-quenching effects, the fluorophores were diluted in a systematic manner by mixing labeled and unlabeled peptides at constant total peptide concentration. Thereafter, the resulting signal intensities were analyzed as a function of fluorophore dilution using the methods described in the Appendix of this paper.

In order to quantitatively analyze the interactions in the membrane by a particle theory, two distinct building blocks are introduced. Whereas the transmembrane peptide results in a disk shape when projected onto the membrane surface, the in-planar orientation is represented by a two-dimensional rod. The sphere (and the corresponding disk in 2D space) is relatively well described by the scaled particle theory,[20,21] and extensions to the rod-shaped hard particle were performed with different approaches.[22,23] Whereas these theoretical models attempt to simplify the description of the membrane interactions, in reality the peptide−peptide, peptide−lipid, and lipid−lipid interactions are highly complex and interlinked. For example, the presence of peptides causes packing defects of the lipids which are distance dependent, and thereby these defects result in an effective interaction between peptides. However, this and electrostatic contributions can be taken into account by introducing an effective peptide−peptide interaction potential.

## RESULTS

In order to allow a precise detection of end-to-end contacts of peptides by self-quenching measurements, the fluorescence label nitrobenzofurazan (NBD) has been covalently linked to the N-terminus of the LAH4 peptide (Figure 1, green structure in the center of the red sphere). Because the fluorescence signal of the NBD chromophore is strongly dependent on the polarity of the surrounding medium,[24] it can also be used to follow membrane insertion of the peptide upon addition of vesicles. Figure 2A,B shows the increase in fluorescence emission at 520 nm of 10 $\mu$M $LAH_4$-NBD upon addition of POPC vesicles at either pH 7 or pH 4, respectively. Furthermore, the emission signal is blue-shifted from a maximum at 536 nm in the absence to about 520 nm in the presence of phospholipid vesicles (not shown).

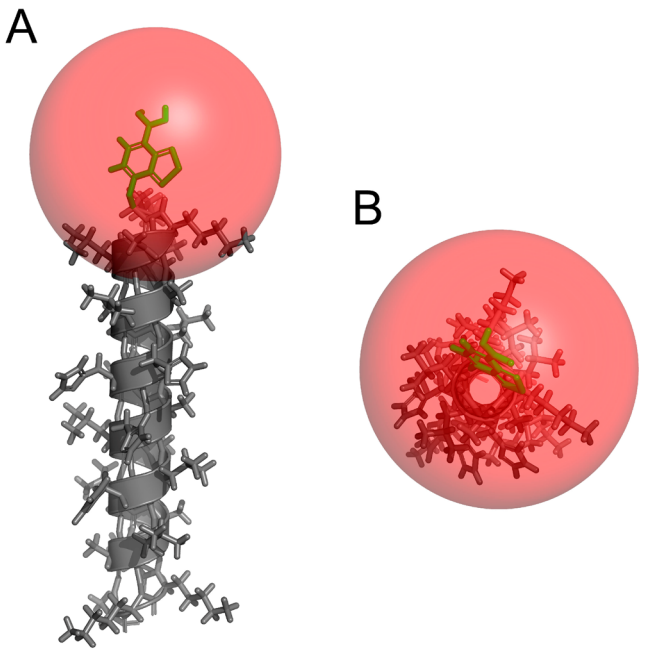


**Figure 1.** Molecular model of NBD-labeled LAH4. The red sphere indicates the critical radius of about 1 nm characterizing the self-quenching properties of NBD.

These spectral changes have been used to estimate the membrane dissociation constants of the peptides, which at pH 7 is 14.2 $\mu$M for POPC vesicles. This pronounced membrane association results in almost complete binding at the first titration step (Figure 2C, open symbols). At pH 4 membrane association is weaker and characterized by an almost linear isotherm up to 100 $\mu$M of POPC (Figure 2C, filled symbols). Analysis of the binding isotherm by a simple membrane partitioning equilibrium results in an apparent dissociation constant of 33.4 $\mu$M.

Self-quenching effects of NBD are well described in the context of NBD-labeled lipids, and the critical radius for self-quenching has been determined to be 1.0 nm,[19] a radius which is indicated in Figure 1 by the red sphere. The self-quenching behavior is characterized by replacing a fraction of the labeled peptide by the fluorophore-free analogue; hence, the label is diluted when at the same time the total peptide concentration remains constant. In the absence of self-quenching the signal intensity is directly proportional to the labeled fraction. In the presence of self-quenching the signal deviates from this linear dependence and is reduced in particular at the higher degrees of labeling. The theory describing this behavior is elaborated in the Appendix of this paper. Figure 2A,B shows the emission signal at 520 nm of NBD-$LAH_4$ in the presence of 10 $\mu$M LAH4 at labeling fractions of 0.2, 0.33, 0.5, 0.67, and 1 for increasing amounts of lipid vesicles. At pH 7 the fluorescence signal exhibits a self-quenching effect already in the absence of lipid vesicles as can be seen from the nonlinear behavior when the fraction of fluorophore labeled peptides is increased (Figure 2A). This is due to the formation of peptide multimers, an effect which will be discussed elsewhere and which has previously been demonstrated by dynamic light scattering investigations.[25] Upon addition of lipid vesicles the signal increases and at the same time shows a characteristic self-quenching effect at lipid concentrations ≤100 $\mu$M. When the lipid concentration is further increased, the dependence on the labeling fraction becomes almost linear when about 20 lipid molecules per peptide are present (200 $\mu$M of POPC).

At pH 4 and in the absence of lipids the signal is directly proportional to the degree of labeling (Figure 2B), indicating that most of the peptide occurs in a monomeric state, in agreement with previous observations.[25] Upon addition of lipid vesicles self-quenching becomes visible up to concentrations of ~100 lipid molecules per peptide (1000 $\mu$M of POPC).

The data of Figure 2A,B were analyzed assuming a Poisson distribution of the number of neighbors within the self-quenching radius (see Appendix). The corresponding fit parameters are represented in Figure 2C,D, respectively. The normalized intensities that would be measured in the absence of self-quenching have been calculated by fitting the data of Figure 2A,B to eqs 2 and 4 (cf. Appendix) and are shown in Figure 2C. This intensity is predominantly influenced by the polarity of the environment[24] and correlates in a direct manner with the fraction of membrane-associated peptides (cf. above). In addition, with the data of Figure 2A,B at hand the high signal


dx.doi.org/10.1021/la500998g | Langmuir XXXX, XXX, XXX−XXX

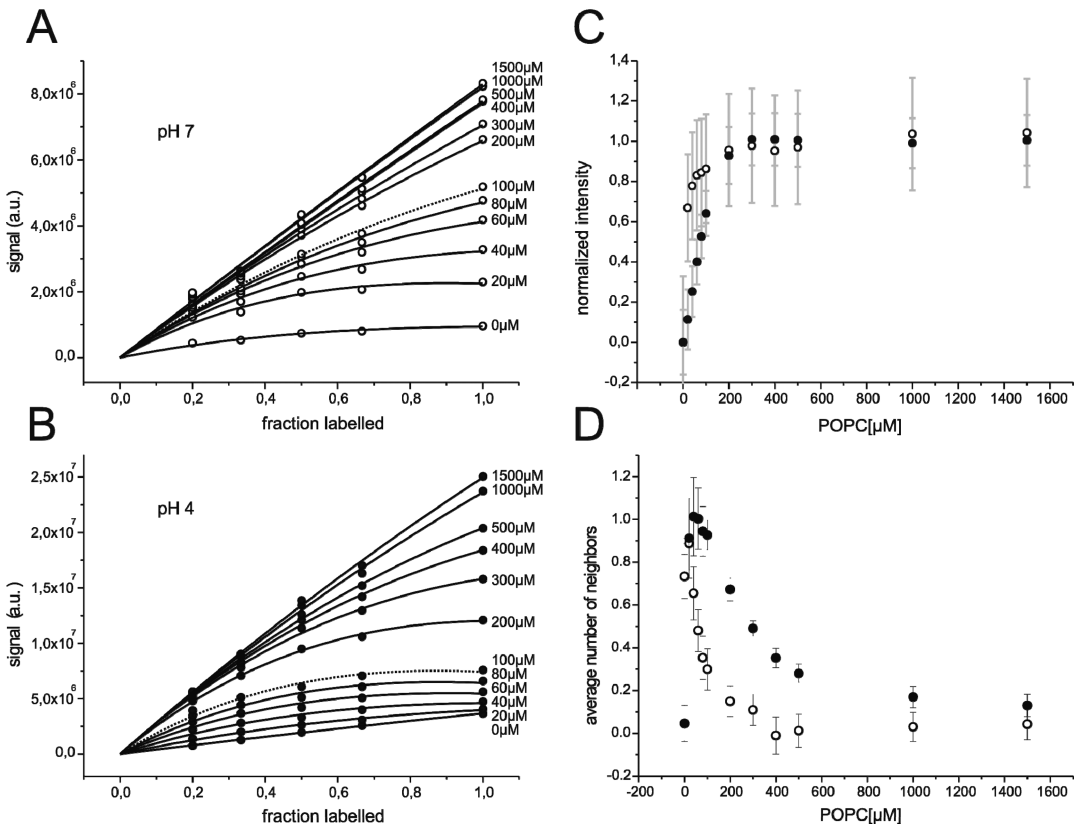


**Figure 2.** Panels A and B show the fluorescence intensity at 520 nm of 10 $\mu$M LAH4 at different fraction of labeling in the presence of increasing amount of small lipid vesicles of POPC at pH 7 (A) and at pH 4 (B). The experimental data (circles) are fitted using a Poisson distribution for the number of neighbors within the self-quenching radius. The dotted line indicates how the fluorescence evolves when the fraction of labeled peptide increases in the presence of 100 $\mu$M POPC. Panels C and D show the fitting parameters used to analyze the data of panels A and B. (C) exhibits the calculated intensities in the absence of self-quenching for pH 7 (open circles) and pH 4 (filled circles). (D) shows the average number of neighbors within the self-quenching radius at pH 7 (open circles) and pH 4 (filled circles).

of the chromophores from the membrane-associated peptides allows the determination of the self-quenching properties of the bound fraction.

Figure 2D exhibits the average number of neighbors within the critical quenching radius. The LAH4 peptide adopts an in-planar orientation at pH 4 and a transmembrane topology at pH 7,[8,26] and there are significant differences in quenching behavior when these two situations are compared to each other (Figure 2D). Whereas the number of neighbors of the transmembrane peptide (open symbols) converges quickly to zero upon addition of vesicles, this value decreases much more slowly in the in-planar case where the maximum number of self-quenching neighbors is obtained at a peptide/lipid ratio of about 1/20 (filled symbols).

In order to further analyze the experimental data, the number of (absorbed) peptides per nm$^2$ of lipid surface has been calculated (Figure 3). The binding isotherm was derived from the changes in signal intensity (e.g., Figure 2C) and used to calculate the amount of bound peptide with respect to the lipid surface. An area per lipid of 68 Å$^2$ was taken into account for this analysis.[27,28] The left-hand column of Figure 3 (panels A, C, and E) shows the average number of neighbors for self-quenching of amino-terminally labeled LAH4 at pH 7 where the helical peptide is transmembrane.[8] Figure 3A represents measurements in the absence of salt (10 mM phosphate buffer; 1 mM EDTA) using POPC vesicles (zwitterionic without net charge). The data of Figure 3C were obtained for POPC/POPG (2/1 mol/mol) vesicles, where the phosphatidylglycerol headgroup carries a negative charge, and the data in Figure 3E are measured using pure POPC vesicles in the presence of 100 mM KCl (10 mM phosphate buffer; 1 mM EDTA) at pH 7. Both the negative surface charge density of the vesicles (Figure 3C) and the presence of salt (Figure 3E) result in a higher number of close-by neighbors consistent with a reduction of repulsive forces between the cationic peptides. As a consequence, the number of neighbors remains high even in the presence of high amounts of lipids (low amount of peptide per area). In order to verify if thermal equilibrium is reached during the titration experiments, a control experiment was performed, where the amount of lipid was added at once (crosses) instead of in a stepwise manner (circles). When the stepwise titration and the single addition of the lipid vesicles are compared to each other, significant differences are observed, indicating that the peptides do not readily redistribute between vesicles (Figure 3C,E), even after 1 day of incubation (not shown). Therefore, we refrained from further analyzing the data obtained for transmembrane LAH4 (pH 7) in POPC/POPG 2/1 or in the presence of salt (Figure 3C,E).

Focusing on the POPC−LAH4 interactions in the absence of salt (Figure 3A), the average number of neighbors is proportional to the surface coverage up to about 0.3 peptides per nm$^2$. In a model of randomly point-shaped particles the expectation value for the number of neighbors ($E_{neighbor}$) is the product of surface coverage $\rho$ and the area in which self-quenching occurs (disk with critical radius for quenching).


dx.doi.org/10.1021/la500998g | Langmuir XXXX, XXX, XXX−XXX

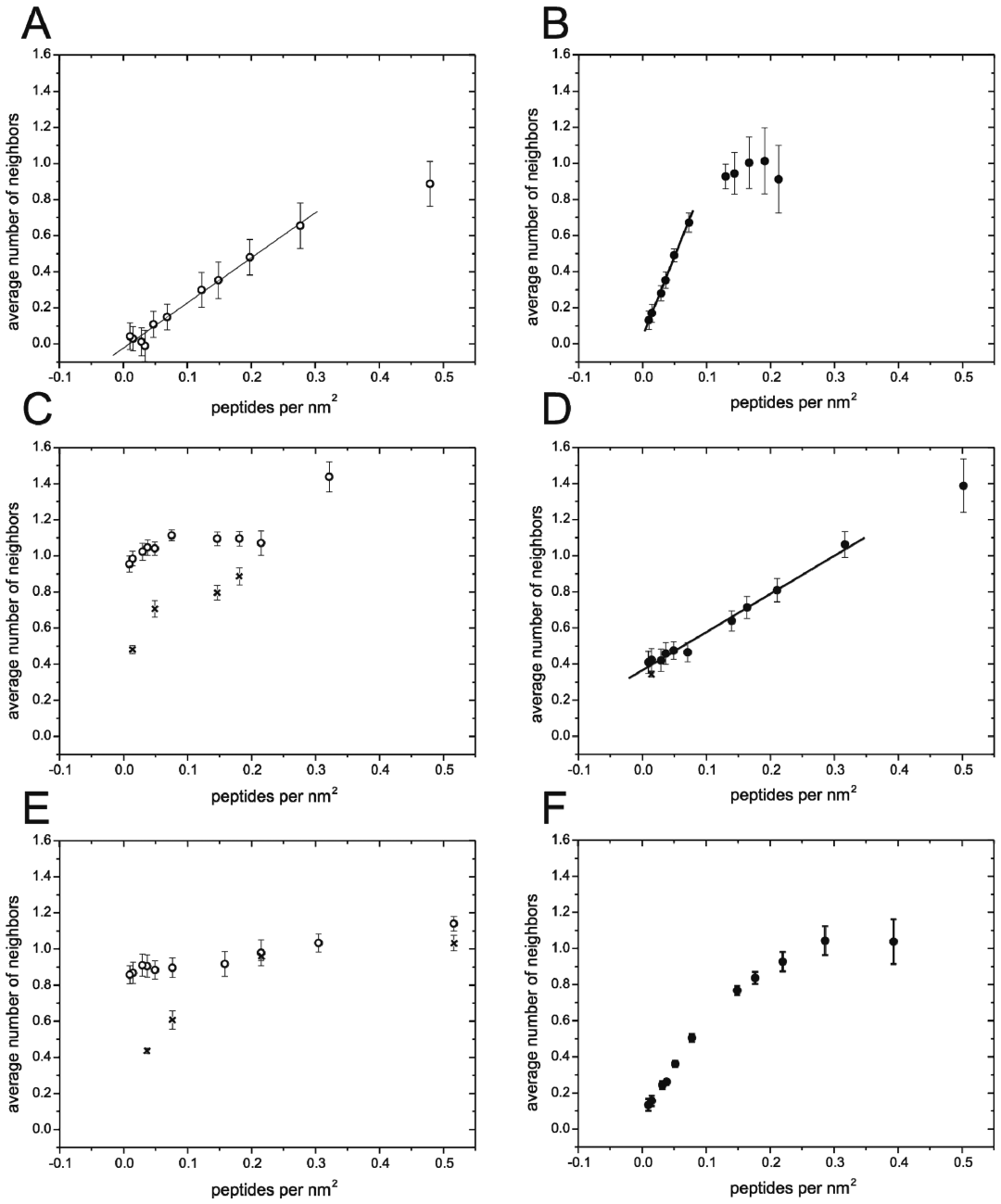


**Figure 3.** Number of neighbors within the self-quenching radius of a peptide is shown as a function of the number of peptides per lipid area projected onto the membrane surface. The left-hand column represents data at pH 7 (A, C, E) and the right-hand column at pH 4 (B, D, F). (A, B) show titration experiments with POPC, (C, D) with POPC/POPG (2/1), and (E, F) with POPC in the presence 100 mM KCl. The crosses in (C, D, and E) correspond to experiments, where the corresponding amount of lipids is added in a single step.

$$E_{\text{neighbor}} = \rho\pi r_0^{\,2}$$

This allows the calculation of a critical quenching radius for the different configurations as displayed in Table 1. The corresponding radius is quite close to 1 nm as expected for the published critical self-quenching radius of NBD.[19]

The right-hand column of Figure 3 (panels B, D, and F) shows the average number of neighbors of NBD-LAH4 at pH 4 where this helical peptide adopts an in-planar configuration. In the absence of salt and in the presence POPC lipid vesicles (Figure 3B) the numbers of neighbors for NBD self-quenching increases very rapidly with a slope of about 15 neighbors nm$^2$/peptide until it saturates at about one neighbor for at 0.1 peptides per nm$^2$. Adding 100 mM of KCl to the sample (Figure 3F) results in a slower increase of the number of neighbors with a saturation at 1 neighbor on average at about 0.3 peptides per nm$^2$.

**Table 1. Increase of the Average Number of Neighbors within Quenching Distance When Compared to the Number of Peptides per Area (Slope) and the Critical Self-Quenching Radius As Deduced from Figure 3**

| | slope nm$^2$/ no. peptides | critical self-quenching radius (nm) |
|---|---|---|
| pH 7 NBD | 2.50 ± 0.37 | 0.89 ± 0.09 |
| pH 7 TAMTA | 0.94 ± 0.35 | 0.55 ± 0.06 |


dx.doi.org/10.1021/la500998g | *Langmuir* XXXX, XXX, XXX−XXX

Using negatively charged vesicles of POPC/POPG (2/1 mol/mol; Figure 3D), the number of neighbors increases in a linear fashion with the surface coverage starting at 0.3 neighbors for very diluted samples up to 1.4 average neighbors for a high surface coverage of 0.5 peptides per nm$^2$. When the lipid vesicles were added in a single step, the observed number of neighbors is only slightly reduced when compared to the titration experiment (Figure 3D, crosses). Hence, the remaining self-quenching at high lipid concentration is indicative of the clustering of the peptide on the membrane surface at thermal equilibrium, rather than a kinetic trapping of the peptides to vesicles.

In a next step the self-quenching assay was performed with LAH4 whose amino-terminus carries a teramethylrhodamine (TAMRA) fluorophore instead of NBD. When the peptides are aligned parallel to the membrane surface (pH 4), fluorescence self-quenching in the presence of POPC and in the absence of salt is below detection (Figure 4A, filled circles). In contrast, the fluorophore attached to the transmembrane peptide (pH 7, Figure 4A, open circles) exhibits self-quenching with a slope of 0.94 ± 0.35 neighbors nm$^2$/peptide. For a randomly distributed sample this corresponds to a self-quenching radius of 0.55 ± 0.06 nm. Hence the radius for self-quenching of TAMRA is about half that of NBD. It should be noted that the signal intensity of TAMRA is largely independent of the polarity of the environment, and therefore the binding isotherms from experiments with NBD labeled peptide were used for this analysis.

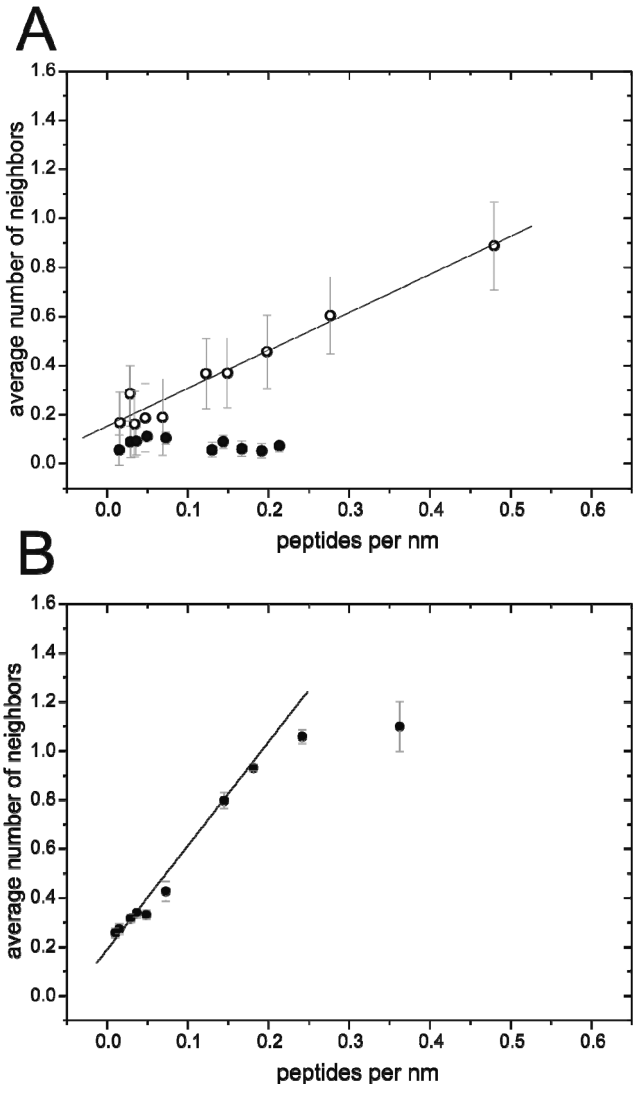


**Figure 4.** Panel A shows the average number of neighbors for TAMRA self-quenching of labeled LAH4 at pH 4 (filled circles) and at pH 7 (open circles). The lipid vesicles consist of POPC. Panel B shows the average number of neighbors for NBD self-quenching of KL14 as a function of the peptide density on the membrane surface at pH 4. The lipid membranes consist of POPC/POPG 2/1.

The NBD-self-quenching assay was extended to a small in-planar model peptide KL14 (KKLLK KAKKL LKKL), which in membranes adopts a helical conformation with a perfect amphipathic distribution of lysine and leucine residues. Since the peptide exhibits only weak binding to neutral lipid vesicles, the experiments were performed in the presence of POPC/POPG (2/1 mol/mol). The number of neighbors for KL14 is increasing fast with the surface coverage (Figure 4B), similar to the behavior of LAH4 in the presence of POPC vesicles and salt (Figure 3F).

## DISCUSSION

The packing of peptides (shaped particles) onto lipid membranes (2D space) is a surprisingly difficult topic for both experimental[29] and theoretical approaches.[30,31] Of special interest are deviations from isotropic arrangements such as nematic phases. In 3D systems a theoretical description of nematic phases of shaped particles is well established in the context of liquid crystals.[32,33] However, in two dimensions the existence of long-range order of hard rods remains subject to controversial discussion. Lipid−peptide systems provide an adequate platform to test the theoretical description for two-dimensional systems of shaped particles for which the existence of phases exhibiting a low degree of order has been predicted.[30,31] In this context we investigated lipid−peptide systems by focusing on the detection of the nearest neighborhood of the peptides using the self-quenching effect of two different fluorescent dyes. In such settings deviations of the nearest-neighbor distribution from an isotropic model provide a good indication for the existence of an ordered phase.

This becomes most obvious when the average number of neighbors is represented as a function of peptides bound per unit lipid area (Figures 3 and 4). In the presence of POPC (no salt) the average number of neighbors in the transmembrane configuration increases in a linear fashion passing through the origin (Figure 3A), a behavior that is expected for a random/isotropic distribution. The slope of the curve is indicative of a self-quenching radius of 1 nm, in agreement with previous data from NBD labeled lipids.[19]

In contrast, strong derivations from an isotropic arrangement are observed at acidic conditions (Figure 3B). Upon shielding of electrostatic interactions by increasing the salt concentration or by adding anionic lipids (Figure 3D,F) a more isotropic distribution is again observed also at low pH.

For TAMRA-labeled LAH4 in the transmembrane configuration the self-quenching effect is weaker (Figure 4A, open circles) when compared to NBD-LAH4 (Figure 3A). The differences in the self-quenching behavior of NBD and TAMRA can be explained by the much smaller critical quenching radius $R_c$ of the latter fluorophore (Table 1). It is remarkable that transmembrane peptides approach each other that closely, since $R_c$ of TAMARA is not much different from the radius of the peptide helix. In the bilayer plane the lipids occupy a surface


dx.doi.org/10.1021/la500998g | Langmuir XXXX, XXX, XXX−XXX

which corresponds to a diameter of about 0.8 nm, indicating that self-quenching within 0.55 nm can only take place when the peptides are in direct contact. Although this may indicate that transmembrane helical oligomers form, it should be noted that our attempts to detect well-defined helical bundles made of LAH4 by single-channel measurements have failed so far [Wrobel, G.; Boheim, G.; Bechinger, B.; Vogel, H., unpublished].

When the peptide coverage of POPC is taken into consideration, the average number of close-by neighbors at the 1 nm quenching radius of NBD increases significantly faster for the in-planar (Figure 3B) when compared to the transmembrane configuration (Figure 3A). In the in-planar orientation the peptide obviously adopts a pattern on the membrane surface, where contacts between the N-termini of the peptides occur more frequently. Possibly the structural arrangement looks similar to self-assembled ellipsoidal particles at water−air and water−oil surfaces.[34] Notably, similar to the observations made here, those structures are also influenced by the charge of the particles. A working model for a system of peptides aligned in a linear fashion is provided in Figure 5.

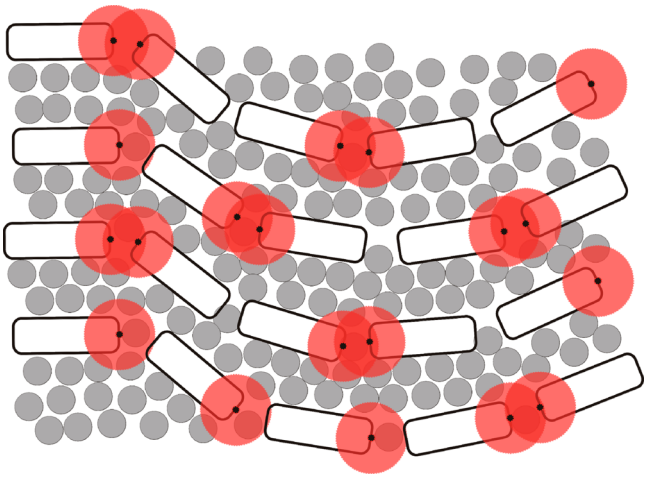

**Figure 5.** Model illustrating an end-to-end alignment of in-planar peptides. The gray circles represent the lipid molecules, the boxes represent the peptides, and the red circles represent the critical radius of the NBD label. The picture corresponds to about 10% of peptide/lipid (mol/mol) or to 0.2 peptides/nm$^2$.

Since the dipolar interactions are largely screened on the membrane surface,[35,36] the direction of the individual peptide within one chain has been chosen random. The number of nearest neighbors is poorly described by a Poisson distribution as half of the chromophores are close to exactly one neighbor. With this model at hand, the data of Figure 2B were reanalyzed by considering that within such membrane assemblies 50% of the chromophores quench when at the same time a fraction of unquenched (free) peptide is present (Figure 6). An enlargement of the lipid surface results in the disappearance of the nematic structures (Figure 6, filled circles) when at the same time the fraction of unquenched peptide increases (Figure 6, open diamonds).

When the LAH4 amphipathic helices were investigated in their in-planar configuration, the TAMRA fluorescence shows no self-quenching effect (Figure 4A, filled circles), whereas the NBD fluorescence exhibits a more pronounced self-quenching behavior when compared to transmembrane NBD peptides

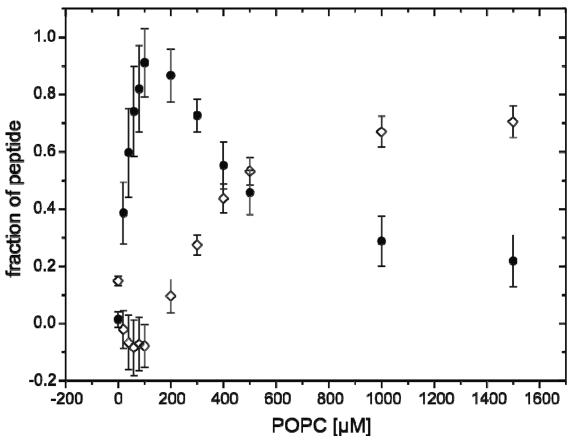


**Figure 6.** Self-quenching data shown in Figure 2B (LAH4 in the presence of POPC without salt) was analyzed by a model where a fraction of peptides occurs in an end-to-end arrangement such as shown in Figure 5 (filled circles) when at the same time a fraction of nonquenching peptide is present (open diamonds).

(Figure 3A,B). Hence, in the in-planar alignment the chromophores (and the amino-terminal ends of the peptides) have a distance between 0.5 and 1 nm. Probably one lipid molecule (diameter ~0.8 nm) is placed between the peptides in the end-to-end arrangement.

When introducing negatively charged lipids (Figure 3D), the slope of the self-quenching function decreases and becomes comparable to the one of the transmembrane peptide in POPC (Figure 3A). Introducing negatively charged lipids destroys the end-to-end contacts and leads to a more random distribution of the chromophores. Upon addition of 100 mM KCl (Figure 3F) an intermediate behavior is observed between the absence of salt (Figure 3B) and the presence of strong electrostatic contributions in POPC/POPG membranes (Figure 3D). Clearly, the presence of salt weakens the end-to-end structure of the peptides. At first glance it seems a paradox that screening the repulsive interactions between the cationic peptides leads to a decrease of the number of neighbors. However, in the context of anisotropic liquid crystal phases of rod like molecules the important role of repulsive electrostatic interactions for the formation of those phases has been shown experimentally[37] and theoretically.[38] This supports the picture of a nematic phase and argues against the formation of simple aggregates, which would be stabilized by salt or anionic lipids.

Self-quenching experiments using the short in-planar peptide KL14 were performed using negatively charged vesicles (POPC/POPG 2/1 mol/mol) (Figure 4B). Because of the weak hydrophobic partitioning of KL14, the apparent membrane association had to be enhanced by the use of negatively charged vesicles. The slope of the curve shown in Figure 4B is closely related to that of the number of neighbors curve for LAH4 in the presence of POPC and salt (Figure 3F). Hence, an end-to-end structural assembly can be detected also for this shorter amphipathic peptide. Whereas the end-to-end supramolecular assembly is lost for LAH4 in the presence of anionic lipids (decreased slope in Figure 3D), it is maintained for KL14 (steep slope in Figure 4B). This is probably due to the higher cationic charge of KL14 (8 Lys and N-terminus out of 14 amino acids: 57% positively charged side chains) when compared to LAH4 (4 Lys and 4 His and N-terminus out of 26 amino acids: 31% charged side chains at low pH). Interestingly, both KL14 and in-plane oriented LAH4 form loose clusters


dx.doi.org/10.1021/la500998g | Langmuir XXXX, XXX, XXX−XXX

even at high dilution in the presence of negatively charged lipids (extrapolating to 0.2−0.3 neighbors) even though their interactions differ when more peptide is added to the membrane (Figures 3D and 4B). Therefore, clustering on the membrane surface might be a common feature of cationic in-planar peptides in the presence of anionic lipids. Furthermore, this behavior might play a role in the antibiotic activity of cationic amphipathic peptides (cf. below).

The data presented in this paper indicate the presence of microscopic order of the membrane adsorbed in-planar peptides. Probably the peptides form a 2D nematic phase[3] such as the one presented in the model presented in Figure 5. Indeed our data are in qualitative agreement with such a model[3] even though a more extensive experimental analysis is required to unambiguously determine all its parameters. A very useful unit is given by the reduced density $\rho = l^2N/A$ as introduced in ref 3, where $l$ is the length of the peptide and N/A the number of peptides per area. Figure 7 shows $\rho$ as a function of the free

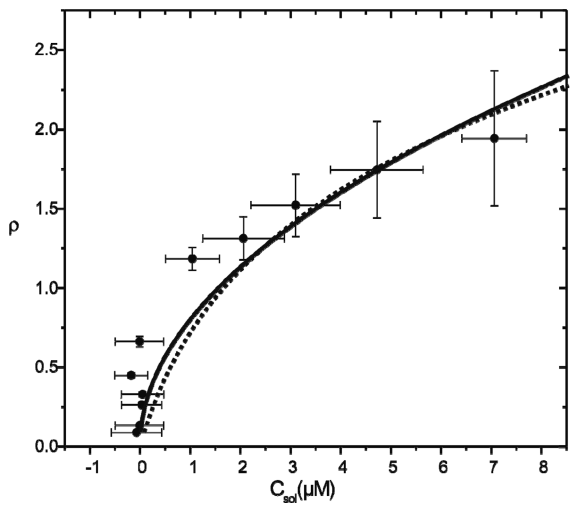


**Figure 7.** Relation beween the reduced density $\rho$ ($\rho = l^2N/A$) and the concentration of free peptide for LAH4 at pH 4 in POPC in absence of salt. The data were fitted with eq 3 for an isotropic configuration (dashed line) leading to a dissociation constant of $K_d = 0.440 \pm 0.034$ $\mu$M and for an anisotropic configuration (solid line) leading to a dissociation constant of $K_d = 0.202 \pm 0.014$ $\mu$M.

LAH4 concentration at pH 4 in the presence of POPC and in the absence of salt. Lines represent binding isotherms for the isotropic and the anisotropic configuration derived by Almeida and Wiegel[3] in a thorough calculation of the partition function,[3] considering the excluded volumes. The values for the dissociation constant is about 1 order of magnitude lower than values obtained by simple membrane-partitioning equations. The simple membrane-partitioning equation obviously underestimates the binding constant by ignoring excluded volumes.

Thus, the experimental data may help to resolve some of the controversial discussions about theoretical aspects in relation to the formation of 2D ordered phases or 2D liquid crystals.[31,39] The strong effect of the electric charge in our experiments is interesting since it plays an important role for the theory of nematic phases in three dimensions[32,40,41] where it lowers the critical concentration for a nematic phase transition.[38,40,42] The phase diagram proposed by Potemkin et al.[40,43] suggests a weakly ordered phase when the parameters of the LAH4 system are taken into consideration. In this analysis LAH4 has a fraction of 0.3 charged amino acids ($\tau$). Furthermore, for a peptide area of about 0.15 nm$^2$ the fraction of peptide volume multiplied with the number of amino acids ($\phi m$) is in the range of 0.4−1.56.

The very existence of an ordered phase of peptides on the surface of lipid membranes potentially plays an important role for the function of membrane peptides. Notably LAH4 peptides and related sequences shown to exhibit pronounced antimicrobial activities[26] are potent compounds for the nonviral transfection[12,44] and viral transduction of nucleic acids.[14] In this context it is noteworthy that LAH4 exhibits a considerably higher activity in antimicrobial assays at pH 5, when the peptide is oriented parallel to the surface, than at pH 7, where it is transmembrane.[26] Bacterial membranes are highly anionic, and the formation of clusters even at low peptide densities (cf. Figure 3D) much increases the local concentration of the peptide and thereby its membrane disruptive activities. A decrease in membrane order and/or changes in macroscopic phase have indeed been observed in the presence of either in-planar or transmembrane alignments.[45−47] Therefore, the packing arrangement of peptides on the membrane surface has to be considered for these biological functions also in the context of a more general model for the peptide−membrane interactions where a number of phase transitions are considered.[47] In contrast, no indications of nematic structures at the membrane surface have been observed in neutral membranes when at the same time the peptide has been shown to be less disruptive for their membrane integrity.[48] This could explain why eukaryotic cells, which expose less anionic lipids to the outer monolayer of their plasma membranes, are not as sensitive to these peptides. In addition, the cluster and patterning of peptides on the membrane surface complements the concept of the well-characterized phase behavior and domain formation ("rafts") of lipids.[49]

## CONCLUSIONS

The fluorescence data presented here show experimental evidence for an anisotropic, mesomorphic arrangement of in-planar peptides on the membrane surface similar to theoretical

**Table 2. LAH4 Arrangements on the Membrane Surface**

| peptide orientation[8] | lipid/buffer | peptide behavior |
|---|---|---|
| transmembrane | POPC in 10 mM phosphate buffer, pH 7 | statistic distribution of the nearest neighbor distance |
| transmembrane | POPC/POPG in 10 mM phosphate buffer, pH 7 | kinetic trapping of the peptides/not in thermal equilibrium |
| transmembrane | POPC in 10 mM phosphate buffer, pH 7, 100 mM KCl | kinetic trapping of the peptides/not in thermal equilibrium |
| in-planar | POPC in 10 mM phosphate, buffer, pH 4 | end-to-end-configuration |
| in-planar | POPC/POPG in 10 mM phosphate buffer, pH 4 | statistic distribution of the fluorophore with clustering for low peptide concentration |
| in-planar | POPC in 10 mM phosphate buffer, pH 4, 100 mM KCl | end-to-end configuration (less stable when compared to the absence of salt) |


dx.doi.org/10.1021/la500998g | Langmuir XXXX, XXX, XXX−XXX

predictions.[3] Electrostatic interactions are identified as a main driving force for the formation of such mesomorphic phases. However, the interplay of electrostatic interactions and shaped particles leads to seemingly "paradoxical" observations such as an increase in intermolecular contact via an mesomorphic phase despite repulsive electrostatic interactions.

## MATERIALS AND METHODS

**Preparation of Small Unilamellar Vesicles.** POPC and POPG (Avanti Polar Lipids, Alabaster, AL) were codissolved in dichloromethane in a small test tube, and the solvent was evaporated under a stream of nitrogen. The remaining traces of organic solvent were removed by high vacuum overnight. The appropriate amount of 10 mM potassium phosphate buffer of appropriate pH containing 1 mM EDTA was added in order to obtain a 10 mM lipid suspension. The samples were first vortexted and then homogenized by four freeze–thaw cycles. Small unilamellar vesicles were produced by tip ultrasonification in an ice bath (Sonoplus 200, Bandelin, Berlin, Germany). Traces of titanium from the sonication tip were removed by centrifugation.

**Peptide Labeling.** The peptide was synthesized as described in ref 8 following the standard Fmoc strategy using a Millipore 9050 peptide synthesizer (Millipore Corp., Bedford, MA) and Fmoc-protected amino acids (Novabiochem/Merck, Nottingham, UK). The labeling of the peptide was performed when still attached to the resin and the side chains protected. Therefore, the N-terminus represented the only free amine after cleavage of the final Fmoc protection group.

**NBD Labeling.** Ten equivalents of 4-chloro-7-nitrobenzofurazan (NBD) (Fluka, Sigma-Aldrich, St. Louis, MO) was dissolved in 50% acetonitrile containing 50 mM $NaHCO_3$, and the resin was incubated for 8 h (typically 2 mL/100 mg resin).[50]

**Tetramethylrhodamine Labeling.** Two equivalents of 5(6)-carboxytetramethylrhodamine (Fluka, Sigma-Aldrich, St. Louis, MO) was dissolved in dimethylformamide in the presence of 2 equiv of diisopropylcarbodiimide (Aldrich, Sigma-Aldrich, St. Louis, MO) and 2 equiv of *N*-hydroxybenzotriazole (HOBT) (Novabiochem/Merck, Nottingham, UK). The resin (typically 100 mg/2 mL) was incubated for 8 h.[51] The labeling was followed by standard TFA cleavage protocol. Peptides were purified by reverse phase HPLC spectroscopy. The identity and purity of the products were confirmed by MALDI mass spectrometry.

**Fluorescence Measurements.** Fluorescence measurements were performed in 10 mM potassium phosphate buffer of the indicated pH in the presence of 1 mM EDTA. Fluorescence spectroscopy was performed using a FluoroLog spectrophotometer (HORIBA, Ltd., Kyoto, Japan) with the polarization filters always at the magic angle. For both NBD and TAMRA fluorescence the slit size was at 3 nm for excitation and emission. For NBD fluorescence the emission was scanned from 470 to 650 nm at an excitation wavelength of 465 nm. For TAMRA the emission was scanned from 525 to 700 nm at an excitation wavelength of 520 nm.

**Calculation of the Reduced Density and Fitting.** The reduced density was calculated using the binding isotherm to calculate the concentration of the bound peptides and assuming an area of 68 Å per lipid molecule and a length of 30 Å for the peptides. The diagram was fitted with a model for isotropic conformation $(c_{sol}/K_d = 2\rho e^{2\rho/\pi})^3$ and with the model of the anisotropic conformation $(c_{sol}/K_d = (e^2\pi\rho^2)/3)$.[3]

## APPENDIX

### Self-Quenching

Samples that exhibit self-quenching properties can be examined by dilution series. For the calculation of the effect of dilution the distribution $K(r,n)$ of $n$ neighbors within the quenching radius $r$ is important. The probability of a nonquenched chromophore at a given fraction of labeled peptide $\lambda$ is then given by

$$P(\lambda, r) = \sum_{n=0}^{\infty} K(r, n)(1 - \lambda)^n \quad (1)$$

The signal intensity of a sample of diluted label is then determined by

$$S(\lambda) = \lambda P(\lambda) \quad (2)$$

For independent (point-shaped) distributed particles one can assume the Poisson distribution

$$K(r, n) = \frac{\delta^n e^{-\delta}}{n!}$$

$$\delta = \rho\pi r^2 \quad (3)$$

where $\delta$ is the expectation value for the number of neighbors derived from the density of particle $\rho$ and the area of the self-quenching.

$$P(\lambda, \delta) = \sum_{n=0}^{\alpha} \frac{\delta^n e^{-\delta}}{n!}(1 - \lambda)^n = e^{-\delta\lambda} \quad (4)$$

In real systems the distribution of the number of neighbors differs from the Poisson distribution since the particles are not independent. If the expectation value for the number of neighbors is small, the difference between the Poisson distribution and a more sophisticated model is small. Furthermore, the application of the Poisson distribution instead of more sophisticated models allows a "model-free" fitting of the data.

In the following different models are described:

In the case of the presence a $n'$-mer (e.g. in solution), the distribution $K(r,n)$ consisting of two nonzero contributions $K(r,0)$ is proportional to the concentration of monomers and $K(r,n' - 1)$ is proportional to the concentration of the $n'$-mer. One can describe the dilution-dependent signal by

$$S_{n'} = \lambda(S_0 + S_{n'}(1 - \lambda)^{n'-1}) \quad (5)$$

At high concentrations on the membrane surface peptide molecules are close due to the restricted area. In this case the $K(r,n)$ is a complex distribution.

For spherical molecules of finite size the maximal number of closest neighbors is six (first coordination shell). For a critical radius for self-quenching $R_a$ in the range of double of the sphere radius this first coordination sphere describes the quenching behavior. Assuming a probability $P_n$ of finding one "place" occupied in the coordination sphere, the distribution $K(n)$ becomes

$$K(n) = \binom{6}{n}(P_n)^n(1 - P_n)^{6-n} \quad (6)$$

For a coordination number of $\alpha$ a more general solution is

$$K(n) = \binom{\alpha}{n}(P_n)^n(1 - P_n)^{\alpha-n} \quad (7)$$

For diluted samples the probability of nonquenched chromophores becomes

$$P(\lambda) = \sum_{n=0}^{\alpha} \binom{\alpha}{n}(P_n)^n(1 - P_n)^{\alpha-n}(1 - \lambda)^n \quad (8)$$

The distribution of the number of neighbors in cases where more than four neighbors can be in the coordination sphere is similar to the Poisson distribution when in average only a few


dx.doi.org/10.1021/la500998g | Langmuir XXXX, XXX, XXX–XXX

neighbors are present. Therefore, fitting with the Poisson distribution is appropriate in this case.

### Radius of Lipid Molecules in the Plane

The average area per POPC molecule is in the range of 68 Å$^2$.[28,52] We assume a tight packing of spherical lipid molecules in the plane. The density of the system is 0.74; i.e., 74% of the space is filled by the special lipid molecules. This leads to a diameter of the lipid molecules in the plane of $d = [(68\ Å^2 \cdot 0.74\pi)/4]^{1/2} \approx 0.8$ nm for a model of spherical disks.

### Abbreviations

NBD-CL, 4-chloro-7-nitrobenzofurazan; NBD, 7-nitrobenzofurazan; POPC, 1-palmitoyl-2-oleoyl-*sn*-3-glycerophosphocholine; POPG, 1-palmitoyl-2-oleoyl-*sn*-3-glycerophosphoglycerol; $LAH_4$, peptide with sequence KKALL ALALH HLAHL ALHLA LALKK A; KL14, peptide with sequence: KKLLK KAKKL LKKL.

## ■ ASSOCIATED CONTENT

### Supporting Information

Supplementary Figure 1: fluorescence intensity of NBD at 520 nm of 10 $\mu$M LAH4 at different fraction of labeling ($x$-axis) in the presence of increasing amount of small lipid vesicles; Supplementary Figure 2: calculated intensities in the absence of self-quenching as result of fitting the data with a Poisson distribution (Supplementary Figure 1). This material is available free of charge via the Internet at http://pubs.acs.org.

## ■ AUTHOR INFORMATION

### Corresponding Author

*Tel +33 3-68-85-13-13; Fax + 33 3-68-85-57-36; e-mail aisenbrey@unistra.fr (C.A.).

### Notes

The authors declare no competing financial interest.

## ■ ACKNOWLEDGMENTS

The work was only possible with the financial support by the Agence Nationale de la Recherche (projects TRANSPEP, ProLipIn, Labex Chemistry of Complex Systems), the RTRA International Center for Frontier Research in Chemistry, Vaincre la Mucoviscidose (French Cystic Fibrosis association), the Fondation pour la Recherche Medicale, the Region Alsace, the CNRS and the University of Strasbourg. We thank the team of Thomas Ebbessen for making his fluorescence spectrometer accessible to us.

## ■ REFERENCES

(1) Singer, S. J.; Nicolson, G. L. The fluid mosaic model of the structure of cell membranes. *Science* **1972**, *175* (23), 720−731.

(2) Engelman, D. M. Membranes are more mosaic than fluid. *Nature* **2005**, *438* (7068), 578−580.

(3) Almeida, P. F. F.; Wiegel, F. W. A simple theory of peptide interactions on a membrane surface: Excluded volume and entropic order. *J. Theor. Biol.* **2006**, *238* (2), 269−278.

(4) Minton, A. P. Adsorption of globular proteins on locally planar surfaces. II. Models for the effect of multiple adsorbate conformations on adsorption equilibria and kinetics. *Biophys. J.* **1999**, *76* (1), 176−187.

(5) Chatelier, R. C.; Minton, A. P. Effect of excluded surface area upon the adsorption of proteins to surfaces. *Biophys. J.* **1996**, *70* (2), TU196.

(6) Zuckermann, M. J.; Heimburg, T. Insertion and pore formation driven by adsorption of proteins onto lipid bilayer membrane-water interfaces. *Biophys. J.* **2001**, *81* (5), 2458−2472.

(7) Aisenbrey, C.; Bechinger, B.; Grobner, G. Macromolecular crowding at membrane interfaces: Adsorption and alignment of membrane peptides. *J. Mol. Biol.* **2008**, *375* (2), 376−385.

(8) Bechinger, B. Towards membrane protein design: pH-sensitive topology of histidine-containing polypeptides. *J. Mol. Biol.* **1996**, *263* (5), 768−775.

(9) Bechinger, B. Insights into the mechanisms of action of host defence peptides from biophysical and structural investigations. *J. Pept. Sci.* **2011**, *17* (5), 306−314.

(10) Kichler, A.; Leborgne, C.; Marz, J.; Danos, O.; Bechinger, B. Histidine-rich amphipathic peptide antibiotics promote efficient delivery of DNA into mammalian cells. *Proc. Natl. Acad. Sci. U. S. A.* **2003**, *100* (4), 1564−1568.

(11) Langlet-Bertin, B.; Leborgne, C.; Scherman, D.; Bechinger, B.; Mason, A. J.; Kichler, A. Design and evaluation of histidine-rich amphipathic peptides for siRNA delivery. *Pharm. Res.* **2010**, *27* (7), 1426−1436.

(12) Zhang, T. T.; Kang, T. H.; Ma, B.; Xu, Y. J.; Hung, C. F.; Wu, T. C. LAH4 enhances CD8+T cell immunity of protein/peptide-based vaccines. *Vaccine* **2012**, *30* (4), 784−793.

(13) Gemmill, K. B.; Muttenthaler, M.; Delehanty, J. B.; Stewart, M. H.; Susumu, K.; Dawson, P. E.; Medintz, I. L. Evaluation of diverse peptidyl motifs for cellular delivery of semiconductor quantum dots. *Anal. Bioanal. Chem.* **2013**, *405* (19), 6145−6154.

(14) Fenard, D.; Genries, S.; Scherman, D.; Galy, A.; Martin, S.; Kichler, A. Infectivity enhancement of different HIV-1-based lentiviral pseudotypes in presence of the cationic amphipathic peptide LAH4-L1. *J. Virol. Methods* **2013**, *189* (2), 375−378.

(15) Boulu, L. G.; Patterson, L. K.; Chauvet, J. P.; Kozak, J. J. Theoretical investigation of fluorescence concentration quenching in two-dimensional disordered-systems - Application to chlorophyll-A in monolayers of dioleylphosphatidylcholine. *J. Chem. Phys.* **1987**, *86* (2), 503−507.

(16) Knoester, J.; Vanhimbergen, J. E. On the theory of concentration self-quenching by statistical traps. *J. Chem. Phys.* **1987**, *86* (6), 3571−3576.

(17) Knoester, J.; Vanhimbergen, J. E. Monte-Carlo simulations on concentration self-quenching by statistical traps. *J. Chem. Phys.* **1987**, *86* (6), 3577−3582.

(18) Baumann, J.; Fayer, M. D. Excitation transfer in disordered two-dimensional and anisotropic 3-dimensional systems - Effects of spatial geometry on time-resolved observables. *J. Chem. Phys.* **1986**, *85* (7), 4087−4107.

(19) Brown, R. S.; Brennan, J. D.; Krull, U. J. Self-quenching of nitrobenzoxadiazole labeled phospholipids in lipid-membranes. *J. Chem. Phys.* **1994**, *100* (8), 6019−6027.

(20) Heying, M.; Corti, D. S. Scaled particle theory revisited: New conditions and improved predictions of the properties of the hard sphere fluid. *J. Phys. Chem. B* **2004**, *108* (51), 19756−19768.

(21) Reiss, H.; Frisch, H. L.; Lebowitz, J. L. Statistical mechanics of rigid spheres. *J. Chem. Phys.* **1959**, *31* (2), 369−380.

(22) Heying, M.; Corti, D. S. The one-dimensional fully non-additive binary hard rod mixture: exact thermophysical properties. *Fluid Phase Equilib.* **2004**, *220* (1), 85−103.

(23) Wouterse, A.; Luding, S.; Philipse, A. P. On contact numbers in random rod packings. *Granular Matter* **2009**, *11* (3), 169−177.

(24) Mazeres, S.; Schram, V.; Tocanne, J. F.; Lopez, A. 7-Nitrobenz-2-oxa-1,3-diazole-4-yl-labeled phospholipids in lipid membranes: Differences in fluorescence behavior. *Biophys. J.* **1996**, *71* (1), 327−335.

(25) Marquette, A.; Mason, A. J.; Bechinger, B. Aggregation and membrane permeabilizing properties of designed histidine-containing cationic linear peptide antibiotics. *J. Pept. Sci.* **2008**, *14* (4), 488−495.

(26) Vogt, T. C. B.; Bechinger, B. The interactions of histidine-containing amphipathic helical peptide antibiotics with lipid bilayers - The effects of charges and pH. *J. Biol. Chem.* **1999**, *274* (41), 29115−29121.

(27) Kucerka, N.; Nieh, M. P.; Katsaras, J. Fluid phase lipid areas and bilayer thicknesses of commonly used phosphatidylcholines as a

function of temperature. *Biochim. Biophys. Acta, Biomembr.* **2011**, *1808* (11), 2761−2771.
(28) White, S. H.; King, G. I. Molecular packing and area compressibility of lipid bilayers. *Proc. Natl. Acad. Sci. U. S. A.* **1985**, *82* (19), 6532−6536.
(29) Heimburg, T.; Marsh, D. Investigation of secondary and tertiary structural-changes of cytochrome-c in complexes with anionic lipids using amide hydrogen-exchange measurements - An FTIR study. *Biophys. J.* **1993**, *65* (6), 2408−2417.
(30) Bates, M. A.; Frenkel, D. Phase behavior of two-dimensional hard rod fluids. *J. Chem. Phys.* **2000**, *112* (22), 10034−10041.
(31) Straley, J. P. Liquid crystals in two dimensions. *Phys. Rev. A* **1971**, *4* (2), 675−681.
(32) Onsager, L. The effects of shape on the interaction of colloidal particles. *Ann. N. Y. Acad. Sci.* **1949**, *51*, 627−659.
(33) Saupe, A.; Maier, W. Eine einfache molekulare Theorie des nematischen kristallinflüssigen Zustandes. *Z. Naturforsch., A* **1958**, *13*, 564−566.
(34) Madivala, B.; Fransaer, J.; Vermant, J. Self-assembly and rheology of ellipsoidal particles at interfaces. *Langmuir* **2009**, *25* (5), 2718−2728.
(35) Sengupta, D.; Behera, R. N.; Smith, J. C.; Ullmann, G. M. The alpha helix dipole: Screened out? *Structure* **2005**, *13* (6), 849−855.
(36) BenTal, N.; Honig, B. Helix-helix interactions in lipid bilayers. *Biophys. J.* **1996**, *71* (6), 3046−3050.
(37) Oster, G. Two-phase formation in solution of tobacco mosaic viruses and the problem of long-range forces. *J. Gen. Physiol.* **1950**, *33* (5), 445−473.
(38) Stroobants, A.; Lekkerkerker, H. N. W.; Odijk, T. Effect of electrostatic interaction on the liquid-crystal phase-transition in solutions of rodlike polyelectrolytes. *Macromolecules* **1986**, *19* (8), 2232−2238.
(39) Fischer, T.; Vink, R. L. C. Restricted orientation "liquid crystal" in two dimensions: Isotropic-nematic transition or liquid-gas one(?). *Europhys. Lett.* **2009**, *85* (5), 56003.
(40) Potemkin, I. I.; Oskolkov, N. N.; Khokhlov, A. R.; Reineker, P. Effect of low-molecular-weight salt on the nematic ordering in solutions of rodlike polyelectrolytes. *Phys. Rev. E* **2005**, *72* (2), 021804.
(41) Yang, D. A.; Venev, S. V.; Palyulin, V. V.; Potemkin, I. I. Nematic ordering of rigid rod polyelectrolytes induced by electrostatic interactions: Effect of discrete charge distribution along the chain. *J. Chem. Phys.* **2011**, *134* (7), 074901.
(42) Potemkin, I. I.; Khokhlov, A. R. Nematic ordering in dilute solutions of rodlike polyelectrolytes. *J. Chem. Phys.* **2004**, *120* (22), 10848−10851.
(43) Potemkin, I. I.; Limberger, R. E.; Kudlay, A. N.; Khokhlov, A. R. Rodlike polyelectrolyte solutions: Effect of the many-body Coulomb attraction of similarly charged molecules favoring weak nematic ordering at very small polymer concentration. *Phys. Rev. E* **2002**, *66* (1), 011802.
(44) Bechinger, B.; Vidovic, V.; Bertani, P.; Kichler, A. A new family of peptide-nucleic acid nanostructures with potent transfection activities. *J. Pept. Sci.* **2011**, *17* (2), 88−93.
(45) Oren, Z.; Shai, Y. Mode of action of linear amphipathic alpha-helical antimicrobial peptides. *Biopolymers* **1998**, *47* (6), 451−463.
(46) Huang, H. W. Molecular mechanism of antimicrobial peptides: The origin of cooperativity. *Biochim. Biophys. Acta, Biomembr.* **2006**, *1758* (9), 1292−1302.
(47) Bechinger, B.; Lohner, K. Detergent-like actions of linear amphipathic cationic antimicrobial peptides. *Biochim. Biophys. Acta, Biomembr.* **2006**, *1758* (9), 1529−1539.
(48) Salnikov, E. S.; Mason, A. J.; Bechinger, B. Membrane order perturbation in the presence of antimicrobial peptides by H-2 solid-state NMR spectroscopy. *Biochimie* **2009**, *91* (6), 734−743.
(49) Simons, K.; Ikonen, E. Functional rafts in cell membranes. *Nature* **1997**, *387* (6633), 569−572.
(50) Dufau, I.; Mazarguil, H. Design of a fluorescent amino acid derivative usable in peptide synthesis. *Tetrahedron Lett.* **2000**, *41* (32), 6063−6066.
(51) Fischer, R.; Mader, O.; Jung, G.; Brock, R. Extending the applicability of carboxyfluorescein in solid-phase synthesis. *Bioconjugate Chem.* **2003**, *14* (3), 653−660.
(52) Kuchinka, E.; Seelig, J. Interaction of melittin with phosphatidylcholine membranes - Binding isotherm and lipid headgroup conformation. *Biochemistry* **1989**, *28* (10), 4216−4221.